

UNIVERSALITY AND SCALING RELATIONS FOR TURBULENT/NON-TURBULENT INTERFACES IN FREE SHEAR FLOWS

Marco Zecchetto¹

¹ LAETA, IDMEC, Instituto Superior Técnico, Universidade de Lisboa, Lisboa, Portugal
e-mail: marco.zecchetto@tecnico.ulisboa.pt

Key words: Computational Fluid Dynamics, Direct Numerical Simulations, Turbulent/non-turbulent interface

Summary. The universality of the statistics of small-scale motions within the turbulent/non-turbulent interface (TNTI) layer that exists at the edges of turbulent free shear flows (i.e. mixing layers) and in turbulent boundary layers is analysed using direct numerical simulations together with conditional statistics. It is shown that at interface level can be found universal aspects in small scales motions, i.e. virtually equal for the same position within the TNTI layer, which implies the universality of the small-scale ‘nibbling’ associated with the turbulent entrainment mechanism.

1 INTRODUCTION

The wake of a car, the jet out of an airplane engine, the air that we exhale, a cloud, are just some examples of turbulent free shear flow. In such flows the central turbulent stream, marked by large vorticity levels, is bounded by fluid in a non-turbulent state, where there is no vorticity (irrotational). Those two regions are separated by a sharp and highly convoluted interface layer named turbulent/non-turbulent interface (TNTI). The detailed shape of interface is continuously deformed by the beneath turbulence and its bulges and indentations evolve as they are carried downstream by the flow. Turbulence imprints the interface and, in turn, the motion of a bulge in the interface influences the irrotational motion outside it. It exist a continuous transition of laminar flow into turbulent one via the turbulent entrainment (TE) process. The turbulent entrainment mechanisms promote a much faster spreading of the shear region compared to solely viscous diffusion. Entering in the turbulent stream a sudden and abrupt change of vorticity, enstrophy, velocity, etc., is measured in the fluid immediately after the TNTI has been crossed. Therefore, entrainment is interlaced both to the TNTI topology and to the dynamics existing in the TNTI proximity but the actual process is still not clarified. Yet, it is accepted that large and small scales motion influence TE. Universal aspects of TE, present and equal in all the flows (e.g. jets, wakes, mixing layer), are most likely to involve the small scales as the large scales motions still carry characteristics of the original turbulence generator.

Chemical mixing, jet propulsion, turbulent combustion, pollutant dispersion, and climatic phenomena are some practical examples in which TE and TNTI dynamics are essential. An active area of research involves controlling the flow by manipulating the natural fluctuations of the interfacial layers through external forcing or local velocity induction. For example, the natural fluctuations and noise produced in the wakes of aircraft wings can be reduced by disrupting

the Kelvin-Helmholtz billows, thereby mitigating noise pollution. A better understanding of these features could foster technological developments (e.g. pollutant emissions in combustion engines, fuel consumption of airplanes) and reduce hazards during extreme events (e.g. volcanic eruptions, unsafe release of chemicals).

In recent years finer experimental measurements and more accurate techniques of numerical simulations prompted the investigation of TE. Information that were previously inaccessible due to the small scale and the rapid evolution of the involved physic are now obtainable.

Direct numerical simulations at high Reynolds number can be carried out using high performance computing (HPC) strategies. All the relevant scales of motion, from the large energy containing scales down to the smallest dissipative scales, are resolved providing detailed insight over the turbulence properties.

Notwithstanding these advancements, the dynamics of turbulent entrainment remain largely elusive.

How strong is the small scale influence in the TNTI region? Can small scales exhibits some degree of universality no matter of the flow type and the Reynolds number? How does the structure of the TNTI evolves?

Such questions have been investigated using temporal direct numerical simulation (DNS).

2 NUMERICAL METHODS

2.1 Direct numerical simulations

The three-dimensional incompressible Navier-Stokes equations for Newtonian fluids are solved numerically. The code used is an in-house Navier-Stokes solver using pseudospectral method (collocation method) for spatial discretization [3], and a third-order explicit Runge-Kutta scheme for the temporal advancement [9]. The domain is a triple periodic cube with sides equal to 2π and the simulations are fully dealiased with the 2/3 rule, and employ $N_1 \times N_2 \times N_3$ collocation points in the x_1 , x_2 , and x_3 directions, respectively [7, 10]. New capability of performing DNS of plane wakes has been added to the bulk of the code.

For the temporal planar jet (*JET*) and planar wake (*WAKE*) simulations, the initial mean velocity is prescribed by an hyperbolic-tangent profile, as in [8],

$$U(x, y, z) = \left(\frac{U_1 + U_2}{2} \right) + \alpha \left(\frac{U_1 - U_2}{2} \right) \tanh \left[\frac{H}{4\theta_0} \left(1 - \frac{2|y|}{H} \right) \right], \quad (1)$$

where x , y , z are the streamwise, normal and spanwise jet directions, respectively, θ_0 is the initial momentum thickness, and U_1 and U_2 are the maximum and minimum initial mean velocities, respectively. Planar jets are obtained by setting the constant α equal to 1 (figure 1a), whereas planar wakes are recovered with $\alpha = -1$.

Afterwards, a three-component velocity fluctuating spectral noise [4] is superimposed by a convolution function that restricts the initial velocity noise to the initial shear layer region of the jet/wake. The maximum amplitude of initial velocity fluctuations is fixed at 5% of the maximum velocity.

The simulation of turbulence in absence of mean shear (SFT) was carried out in a periodic box of size $2\pi \times 2\pi \times 2\pi$ from an initial turbulent field issued from a previously run DNS of forced homogeneous isotropic turbulence (HIT), using the forcing scheme by Alvelius [1] with a peak forcing concentrated in the 3 wavenumbers centered at $k_p = 2$ with a resolution of $k_{max}\eta = 1.1$

Table 1: Summary of the temporal simulations of shear free turbulence (SFT), planar jets (JET) and planar wakes (WAKE). $(N_x \times N_y \times N_z)$ is the number of collocation points used in the streamwise (x), normal (y), and spanwise (z) directions, respectively; $(L_x \times L_y \times L_z)$ is the size of the computational domain in the same directions; Re_H is the initial Reynolds number for the temporal jet and wake simulations; $\langle Re_\lambda \rangle_T$ is the Reynolds number based in the Taylor micro-scale in the turbulent core region of the flow computed from conditional statistics (means) taken from an instantaneous field at the self-similar regime; Δ_x/η is the resolution normalised by the Kolmogorov micro-scale, where η is taken from the centreline of the flow (at the middle plane of the turbulent core region).

	Re_H	$\langle Re_\lambda \rangle_T$	$N_x \times N_y \times N_z$	$L_x \times L_y \times L_z$	Δ_x/η
SFT ₂₀₂	—	202	$1536 \times 1536 \times 1536$	$2\pi \times 2\pi \times 2\pi$	1.1
JET ₁₉₃	8000	193	$1536 \times 1536 \times 768$	$7H \times 7H \times 3.5H$	1.0
JET ₂₇₆	12000	276	$2048 \times 2048 \times 1024$	$7H \times 7H \times 3.5H$	1.1
WAKE ₂₅₉	16000	259	$2048 \times 2048 \times 512$	$7H \times 7H \times 1.75H$	1.3
WAKE ₂₆₆	16000	266	$2048 \times 2048 \times 512$	$7H \times 7H \times 1.75H$	1.4
WAKE ₃₂₈	18000	328	$4096 \times 4096 \times 1024$	$10H \times 10H \times 2.5H$	1.0

[5]. The SFT simulation starts with an initial transient (intermediate) simulation, where the initial velocity fields from the HIT are convoluted by a profile that essentially maintains the velocity of the HIT simulation in $-\pi/4 \leq y \leq +\pi/4$, while artificially setting to zero the velocity field in the region $|y| \geq \pi/4$. The convolution profile used is similar to the hyperbolic tangent profile used in equation 1 so that the initial transition between the HIT and the $u_i(x, t) = 0$ region is smooth. The time step is maintained very small during this intermediate simulation (roughly equal to 1/10 of the one used in the HIT simulations).

2.2 Conditional statistics

Relevant statistics in each simulation are obtained both along time and at particular selected instants of interest. On those instants the outer surface of the interface layer is identified as a vorticity magnitude iso-surface. Vorticity is a key quantity in our analysis as the irrotational region has a no vorticity whereas it is very present inside the turbulent stream.

The thin and highly convoluted nature of the TNTI poses practical difficulties in analysing the flow dynamics in its proximity. First of all, data collected at fixed position near the TNTI, for example at a fixed transversal distance from the centre plane of a plane jet (figure 1b), inevitably mix samples from irrotational and turbulent region. This affects the statistical analysis smearing out the local gradients and shrouding underlying dynamics. Secondly, the interface sharpness and the abrupt evolution of the flow dynamics demand high resolution and accuracy in measurements and simulations. Those two factors have been limiting the investigations until recently. Beginning with Bisset et al. [2], researchers have used local reference frames constructed onto the TNTI to extract an interface flow field description that cannot be achieved in the laboratory reference frame alone. With this new metric, named conditional statistic, data

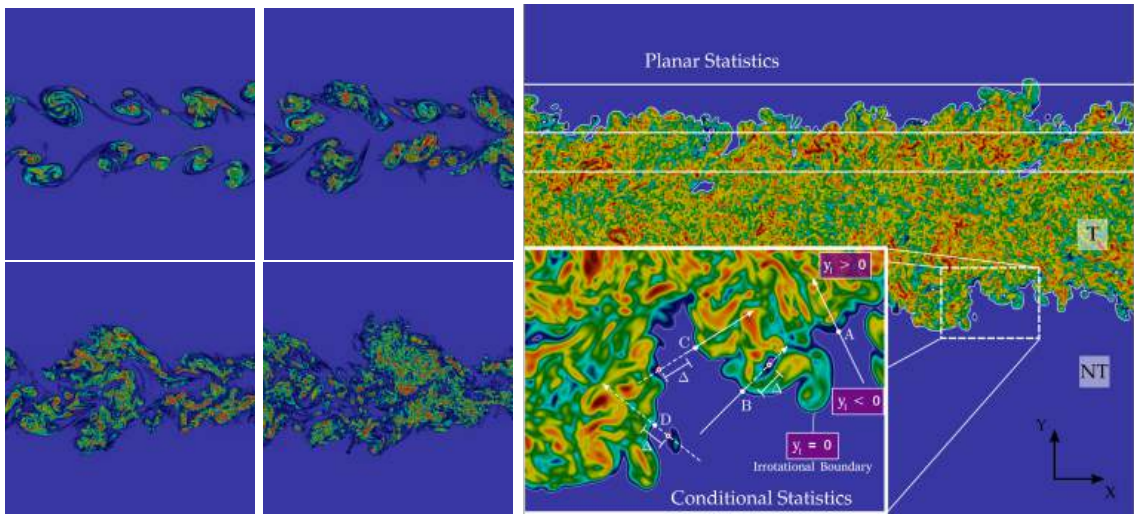


Figure 1: (a) Vorticity magnitude contour of temporal evolving planar jet DNS in 4 instants. (b) Schematic of conditional statistics in a planar wake. Depicted the local reference axis at different points of origin (A-D).

sampling is performed in relation to the distance from the irrotational boundary that becomes the reference surface.

Using this surface as a new reference, conditional statistics are calculated rearranging data samples as function of the distance from the interface (figure 1b).

The procedure used to obtain conditional statistics follows roughly three steps [6, 11]:

- the location of the outer edge of the TNTI – the irrotational boundary (IB) - which consists of an isosurface of very low vorticity magnitude $\omega_{th} = (\omega_i \omega_i)^{1/2}$, is detected by analysing a histogram of the turbulent flow fraction of the flow;
- a local three-dimensional (3-D) axis is then placed with its origin at each of the IB, aligned in the normal direction of the local outer boundary surface;
- the conditional statistics are then computed as a function of the distance to the TNTI layer using this (local) 3-D normal to the irrotational boundary surface. Indeed, any flow quantity of interest is collected at fixed distances y_I by tri-linear interpolation, into a grid defined on this local 3-D normal. The normal points towards the interior of the turbulent core region, so that $y_I < 0$ and $y_I > 0$ correspond to the irrotational and turbulent regions, respectively (the IB is fixed at $y_I = 0$).

Those powerful numerical tools fostered the detailed investigation of the TNTI in plane jets, plane wakes and turbulence in absence of mean shear.

3 RESULTS

The universality of the statistics of small-scale motions within the turbulent/non-turbulent interface layer is analysed using direct numerical simulations of turbulent jets, wakes and turbulent fronts evolving without mean shear. The Taylor based Reynolds number (Re_λ) of the

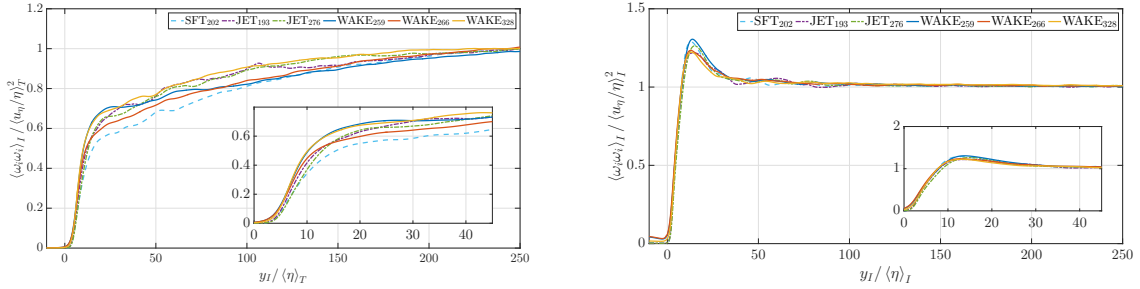


Figure 2: (a) Vorticity magnitude contour of temporal evolving planar jet DNS in 4 instants. (b) Schematic of conditional statistics in a planar wake. Depicted the local reference axis at different points of origin (A-D).

simulations is above of approximately 200, which is required to obtain the asymptotic solutions of the TNTI dynamics [7], while the resolution is comparable to the Kolmogorov micro-scale η (with $\eta = \frac{\nu^{3/4}}{\varepsilon^{1/4}}$ where ν is the kinematic viscosity and $\varepsilon = 2\nu S_{ij} S_{ij} = \frac{\nu}{2} \left(\frac{\partial u_i}{\partial x_j} + \frac{\partial u_j}{\partial x_i} \right)^2$ is the kinetic energy dissipation rate).

A series of conditional mean profiles, denoted by $\langle \cdot \rangle_I$, are obtained as a function of the distance from the IB, which marks the outer surface of the TNTI layer. These profiles showed that the Kolmogorov velocity and length scale are approximately constant and equal to the values deep inside the turbulent core of the flow for the entirety of the TNTI layer changing only close to the IB, for distances of less than $\approx 5\eta$ from the IB position [10].

For all the flow types and Reynolds numbers analyzed the conditional mean enstrophy profiles ($\langle \omega_i \omega_i \rangle_I$, where $\omega_i = \epsilon_{ijk} \frac{\partial u_j}{\partial x_k}$ where ϵ_{ijk} is the Levi-Civita tensor) normalized by the turbulent core Kolmogorov velocity and length scales exhibit a sharp enstrophy jump near the IB, followed by a slower increase moving into the turbulent core region, with different profiles for the different cases (figure 2a). In contrast, the normalization of the same quantity using the local Kolmogorov velocity and length scales shows that all the mean enstrophy profiles collapse into a single curve (figure 2b). The peculiar ‘bump’ observed in these profiles at a distance of $\approx 10\eta$ from the IB, representing a deviation of the flow from a state of local homogeneity in that region, can be explained by the existence of regions of low pressure caused by a row of intense (tube-like) vorticity structures with axes aligned tangent to the isosurface defining the IB. The conclusion is that the profiles, and so the enstrophy evolution, are universal, i.e. virtually equal for the same position within the TNTI layer, which implies the universality of the small-scale ‘nibbling’ associated with the turbulent entrainment mechanism. Indeed, the conditional mean profiles of enstrophy, that represents small-scales motions, when normalised by the local mean Kolmogorov velocity and length scales becomes independent on both flow type and Reynolds number.

Furthermore, the scaling of the turbulent/non-turbulent interface at high Reynolds numbers is investigated by using direct numerical simulations (DNS) of temporal turbulent planar jets (PJET) and shear free turbulence (SFT), with Reynolds numbers in the range $142 \leq Re_\lambda \leq 400$.

The local extent of the TNTI (δ_ω) is defined as the distance between the IB ($y_I = 0$) and this first local vorticity maximum (figure 3a). The mean values of the thickness ($\langle \delta_\omega \rangle$) are computed from the local values of δ_ω .

Figure 3b shows the mean thickness of the TNTI $\langle \delta_\omega \rangle$, normalised by the Kolmogorov micro-

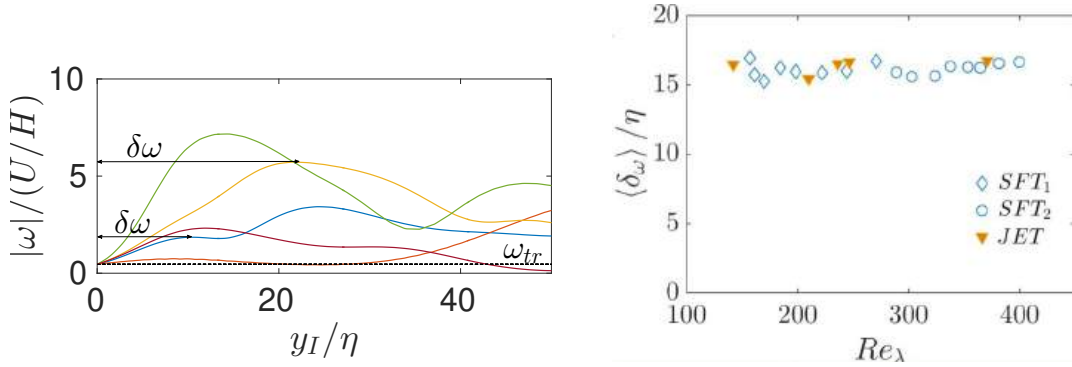


Figure 3: (a) Example of single conditional profile of $|\omega|$ in the case of plane jet normalised with the mean velocity and initial jet width; (b) normalised with the mean local Kolmogorov velocity and length scale, computed at each coordinate y_I , $\langle \eta \rangle_I$ and $\langle u_\eta \rangle_I$, respectively. The insets shows the amplified region near $y_I = 0$.

scale η expressed as a function of the Reynolds number. It is clear that the mean thickness of the TNTI $\langle \delta_\omega \rangle$ tend to a constant value at high Reynolds numbers, when normalised by the Kolmogorov micro-scale η . In other words, the mean thickness of the TNTI becomes independent of the Reynolds numbers when it is sufficiently high, i.e. it scale with the Kolmogorov length scale, $\delta_\omega \sim \eta$. The precise value of $\langle \delta_\omega \rangle$ varies between $15.4 \leq \frac{\langle \delta_\omega \rangle}{\eta} \leq 16.8$ (figure 3b).

Physically it can be explained by the fact that at higher Reynolds numbers the large eddies tend to be more fragmented and all we are left with is small-scale intense ‘worms’. Therefore, it is likely that the same scaling should be observed in TNTIs from other flows, i.e. this suggests that TNTIs from other flow types, e.g. mixing layers and boundary layers, should also scale with the Kolmogorov micro-scale η , provided the Reynolds number is sufficiently high, so that large-scale inhomogeneities are no longer reflected in the small scale vortex characteristics at the TNTI.

4 CONCLUSIONS

The universality of the statistics of small-scale motions is the cornerstone of the theory of turbulence and can take many different forms in fully developed turbulence. Here presented evidences of a similar universality in the small-scale statistics near the turbulent/non-turbulent interface (TNTI) layer, which exists at the edges of many flows such as turbulent jets, wakes, and mixing layers, as well as in turbulent boundary layers. The small scale variables analyzed here are the basic variables typically considered when assessing the small scales of motion in turbulent flows: vorticity and related quantities.

The main tools of the research are direct numerical simulations (DNS) of temporal turbulent planar jets (JET), planar wakes (WAKE), and turbulence in the absence of mean shear (SFT), along with conditional statistics to analyze the dynamics near the turbulent/non-turbulent interface.

Conditional mean enstrophy profiles have been normalized by both the turbulent core Kolmogorov velocity and length scales, and by the local Kolmogorov velocity and length scales. Using this second normalization, all the mean enstrophy profiles collapse into a unique curve, demonstrating that the evolution of enstrophy, from the TNTI to the turbulent core region of

different flows over a wide range of Reynolds numbers, is the same, i.e., universal. Furthermore, the small scales of motion near the TNTI layer are statistically very close to homogeneous, except for a distance of about 10 Kolmogorov length scales from the outer surface of the TNTI layer.

Moreover, the scaling of the turbulent/non-turbulent interface at high Reynolds numbers is investigated by using DNS of temporal turbulent JET and SFT, with Reynolds numbers in the range $142 < Re_\lambda < 400$. It is found that the mean thickness of the TNTI ($\langle \delta_\omega \rangle$) scales with the Kolmogorov micro-scale η , with a particular scaling constant ranging between $15.4 < \langle \delta_\omega \rangle / \eta < 16.8$.

FUNDING

M. Zecchetto acknowledges Fundação para a Ciência e a Tecnologia (FCT) for funding through project 10.54499/SFRH/BD/144291/2019.

References

- [1] K. Alvelius. “Random forcing of three-dimensional homogeneous turbulence”. In: 11(7) (1999), pp. 1880–1889.
- [2] D. K. Bisset, J. C. R. Hunt, and M. M. Rogers. “The turbulent/non-turbulent interface bounding a far wake”. In: 451 (2002), pp. 383–410.
- [3] C. Canuto et al. *Spectral Methods in Fluid Dynamics*. Scientific Computation. Springer Berlin Heidelberg, 2012. ISBN: 9783642841088.
- [4] M. Lesieur, S. Ossia, and O. Métais. “Infrared pressure spectra in 3D and 2D isotropic incompressible turbulence”. In: 11 (1999), pp. 1535–1543.
- [5] B. Perot and P. Moin. “Shear-free turbulent boundary layers. Part 1. Physical insights into near-wall turbulence”. In: 295 (1995), pp. 199–227.
- [6] T. S. Silva and C. B. da Silva. “The behaviour of the scalar gradient across the turbulent/non-turbulent interface in jets”. In: 29 (2017), p. 085106.
- [7] T. S. Silva, M. Zecchetto, and C. B. da Silva. “The scaling of the turbulent/non-turbulent interface at high Reynolds numbers”. In: *Journal of Fluid Mechanics* 843 (2018), pp. 156–179. DOI: <https://doi.org/10.1017/jfm.2018.143>.
- [8] S. Stanley, S. Sarkar, and J. P. Mellado. “A study of the flowfield evolution and mixing in a planar turbulent jet using direct numerical simulation”. In: 450 (2002), pp. 377–407.
- [9] J. H. Williamson. “Low-Storage Runge-Kutta schemes”. In: 35 (1980), pp. 48–56.
- [10] M. Zecchetto and C. B. da Silva. “Universality of small-scale motions within the turbulent/non-turbulent interface layer”. In: *Journal of Fluid Mechanics* 916 (2021), A9. DOI: [10.1017/jfm.2021.168](https://doi.org/10.1017/jfm.2021.168).
- [11] M. Zecchetto et al. “Turbulent/non-turbulent interfaces in equilibrium and non-equilibrium regions in the absence of mean shear”. In: *International Journal of Heat and Fluid Flow* (2023). DOI: <https://doi.org/10.1016/j.ijheatfluidflow.2023.109198>.